Plant functional types, nutrients and hydrology drive carbon cycling along a transect in an anthropogenically altered Canadian peatland complex

Sina Berger[1,2,3], Leandra Praetzel[1,2], Marie Goebel[1,2], Christian Blodau[1,2,†], Klaus-Holger Knorr[1]

5 [1] University of Muenster, Institute of Landscape Ecology, Ecohydrology and Biogeochemistry Group, Heisenbergstraße 2, 48149 Muenster, Germany

[2] University of Guelph, School of Environmental Sciences, 50 Stone Road East, Guelph, Ontario, N1G 2W1, Canada

[3] Karlsruhe Institute of Technology, Institute of Meteorology and Climate Research (IMK-IFU), Kreuzeckbahnstraße 19, 82467 Garmisch-Partenkirchen, Germany

10 *Correspondence to*: Sina Berger (geflecksterschierling@gmx.de), Klaus-Holger Knorr (kh.knorr@uni-muenster.de)

Abstract. Peatlands play an important role in global carbon cycling, however, the response of peatland carbon fluxes to anthropogenically changed hydrologic conditions and long-term infiltration of nutrients is still understudied. Along a transect of 4 study sites, spanning from largely pristine to strongly altered conditions within the Wylde Lake peatland complex in Ontario (Canada), we monitored carbon dioxide (CO_2) and methane (CH_4) fluxes at the soil/atmosphere interface 15 and DIC and CH_4 concentrations in the peat profiles from April 2014 through September 2015. Moreover, we applied δ^{13}C-CH_4 and δ^{13}C-CO_2 stable isotope abundance analyses to examine CH_4 and CO_2 production and consumption as well as the dominant CH_4 emission pathways during the growing season of 2015. We found that a graminoid-moss dominated site, which was exposed to wet conditions and long-term infiltration of nutrients, was a great sink of CO_2 (2260 ± 480 g CO_2 m^{-2}) but a great source of CH_4 (61.4 ± 32 g CH_4 m^{-2}). Comparably low δ^{13}C-CH_4 signatures (-62.30 ±5.54 ‰) indicated only low 20 mitigation of CH_4 emission by methanotrophic activity here. On the contrary, a shrub dominated site, which has been subjected to similarly high moisture conditions and loads of nutrients, was a much weaker sink of CO_2 (1093 ± 794 g CO_2 m^{-2}) as compared with all other sites. The shrub dominated site featured notably low DIC concentrations in the peat as well as comparably ^{13}C enriched CH_4 (δ^{13}C-CH_4: -57.81 ±7.03 ‰) and depleted CO_2 (δ^{13}C-CO_2: -15.85 ± 3.61 ‰) in a more decomposed and surficial aerated peat, suggesting a higher share of CH_4 oxidation. Plant mediated transport was the 25 prevailing methane emission pathway throughout the summer of 2015 among all sites, even where graminoids covered only 10 % of the area. Our study provides insight into the accelerated carbon cycling of a strongly altered peatland and our results supported earlier findings, that strongly altered, shrub dominated peatlands may turn into weak carbon sinks or even sources, while a graminoid-moss dominance may maintain the peatland's carbon storage function.

1 Introduction

Since the end of the last glaciation, northern peatlands have played an important role in global carbon (C) cycling by storing atmospheric carbon dioxide (CO_2) as peat, but also emitting significant amounts of C as methane (CH_4) (Succow and Joosten, 2012).

5 Carbon sequestration and CO_2 and CH_4 release are driven by numerous processes and the accumulation of peat results from only a small imbalance of photosynthetic carbon uptake over respiratory losses. CO_2 can be released through autotrophic and heterotrophic respiration under aerobic and anaerobic conditions (Limpens et al., 2008). Controls on heterotrophic respiration have been intensively studied and depend e.g. on temperature, substrate quality, energetic constraints and other

10 factors (Blodau, 2002). Methanogenesis is strictly limited to anaerobic conditions (Conrad, 2005). Due to thermodynamic controls, CH_4 production is only competitive upon depletion of alternative, energetically more favorable electron acceptors for anaerobic respiration, such as nitrate, iron, sulfate or oxidized humics (Blodau, 2002; Klüpfel et al., 2014).

Ample of abiotic and biotic factors have been identified to further influence production and emission of CH_4 on the field scale, such as water level, temperature of air, soil and water as well as provision of fresh substrates or inhibitors through root

15 exudates, which is coupled to photosynthetic activity (e.g. Shannon and White, 1994; Moore and Basiliko, 2006; Dorodnikov et al., 2011). CH_4 is released to the atmosphere by three different processes: i) through diffusion through the acrotelm, which is a relatively slow process, ii) through ebullition, i.e. a fast evasion of methane bubbles, and iii) through fast molecular diffusion or pressurized throughflow convection through aerenchyms of vascular plants (Morris et al., 2011; Schütz et al., 1991; Whiting and Chanton, 1996; van den Berg et al., 2016; Hornibrook et al., 2009). Due to the slow

20 diffusion of methane in peat, up to 100 % of diffusive CH_4 is oxidized in the acrotelm before it reaches the atmosphere, while the fast processes effectively bypass oxidation and thus contribute a major fraction to observed fluxes (Whalen et al., 1990; Whalen, 2005). Therefore, a change in vascular plant cover or changes in the peat structure due to altered litter inputs and stronger decomposition can be expected to affect methane emissions.

Since changes in distribution of plant functional types (PFT) were shown to lead to changes not only in methane emission

25 bus also in overall carbon cycling (Strack et al., 2006; Breeuwer et al., 2009, Kuiper et al., 2014), interactions between plants, microbes and peat are increasingly being elaborated. For example, in the context of climate warming, an increasing ericaceous shrub cover was associated with increasing polyphenol content in plant litter and pore-water, as well as increasing phenol oxidase activity. Moreover, a higher release of labile C from vascular plant roots was observed (Bragazza et al., 2013, Bragazza et al., 2015) and plant–derived low molecular organic compounds enhanced peatland microbial activity (Robroek

30 et al., 2015). Also, long term nutrient inputs into peatlands are expected to change vegetation and as a consequence carbon cycling: For example, after a 10-15 years fertilization experiment in a bog in eastern Canada, both availability of substrates for microbes and activity of microbial enzymes were found to be altered (Pinsonneault et al., 2016). Thereby, the PFT of

shrubs could apparently buffer more effectively changed environmental conditions, as the bulk chemical composition and nutrient contents of litter seemed largely constant over a broad range of conditions with changed environmental resources (Wang et al., 2016).

Nevertheless, there is still a gap of knowledge in terms of interactions and feedbacks between plants and peat, especially

5 under in-situ conditions. There is still only a poor understanding of the interplay of PFTs, substrate quality, and anoxic-oxic conditions, and of how exchange of CO_2 and CH_4 at the soil/atmosphere-interface would eventually be affected.

To address this research gap, we studied the interaction between cover of certain PFTs, CO_2 and CH_4 emissions and peat quality along a gradient of nutrient availability through a nearby water reservoir. Thereby, we compared a shrub-moss-dominated site vs. graminoid-moss-dominated sites vs. a site with a mixture of mosses, shrubs, graminoids and trees.

10 Moreover, to address changes in methanogenic pathways and to study predominant pathways of emission, we assessed seasonal variation in $\delta^{13}C$ of CH_4 in peat profiles and in CH_4 surface fluxes along a transect of study sites in the Wylde Lake peatland in Ontario, Canada. Wylde Lake peatland has recently been shown to experience strong changes in vascular plant coverage and strongly increased peat accumulation as a response to long term enhanced nutrient infiltration and changed hydrological conditions (see Berger et al., (submitted for publication)), so that different areas of the peatland can serve as

15 sentinels of future responses of peatlands to land use changes.

We hypothesized that 1) in the peatland periphery, where nutrient input is greatest, C-cycling is accelerated as indicated by more decomposed bulk peat along peat profiles, 2) altered abundance of PFTs cause concomitant differences in C-dynamics such as high CO_2 uptake at the shrub dominated sites, and greatest CH_4 emissions at graminoid dominated sites. Moreover, 3) the dominant CH_4 emission pathway is plant-dominated transport where aerenchymatous graminoids are abundant while

20 under predominance of shrubs diffusion is relatively more important for CH_4 emission and thus methanotrophic modification of fluxes is more likely.

2 Methods

2.1 Description of the study area and study sites

Wylde Lake peatland has been described in detail in Berger et al., (submitted for publication). In brief, it is located in the

25 southeastern part of Ontario, 80 km northwest of the city of Toronto (43.920361° N, 80.407167° W) (Fig. 1). The Wylde Lake peatland area is part of the Luther Lake Wildlife Management Area and located in its south-southeastern part. Climate is cool temperate, average July temperature is 19.1 ° C, average January temperature is −8.0 ° C and the mean annual temperature is about 6.7 ° C. Annual precipitation amounts to 946 mm, with the major portion falling in summer (1981 to 2010, Fergus Shand Dam, National Climate Data and Information Archive, 2014).

30 Peat formation started about 9000 years before present on calcareous limnic sediments and total peat depth today is about 5 meters.

For flood control and water management, the "Luther Lake" reservoir, neighboring Wylde Lake peatland, has been created in 1954. Through flooding of the reservoir, Wylde Lake peatland has been exposed to altered hydrological conditions and infiltration of nutrients since the 1950s.

Regarding Wylde Lake peatland´s vegetation, its shoreline to the Luther Lake reservoir is nowadays dominated by a floating
5 mat of cattail (*Typha latifolia* and *T. angustifolia*). Adjacent to that, the northern periphery of the peatland, which may be regarded as an open bog – poor fen transition area, is characterized by a belt of pronounced hummocks, which rise up to 0.8 m above narrow, small hollows. Those hummocks are several meters long and accommodate a dense cover of gigantically grown *Myrica gale* individuals, which suppress growth of underlying *Sphagnum* mosses. The vegetation of the adjacent more pristine open bog south is composed of dominant *Sphagnum* mosses (e.g., *S. magellanicum*, *S. cuspidatum*, *S. fuscum*),
10 shrubs (e.g., *Myrica gale*, *Vaccinium spp.*, *Chamaedaphne calyculata*, *Rhododendron groenlandicum*, *Kalmia polifolia*, *Andromeda polifolia*), graminoids (*Cyperaceae*, e.g., *Eriophorum spp., Carex spp.*) and few scattered herbaceous plants (e.g. *Sarracenia purpurea, Maianthemum trifolium*); the vegetation structure is rather typical of bog vegetation. The micro topography is a typical bog´s mosaic of hummocks, hollows and lawn-like grass carpets. The treed bog area to the south is dominated by black spruce (*Picea mariana*), tamarack (*Larix laricina*), pine trees (*Pinus spp.*) and individuals of swamp
15 birches (*Betula pumila*).

Four intensively investigated measurement sites (Fig. 1) were arranged along a transect stretching from the shoreline of the Luther Lake reservoir about ~1 km to the south into the central treed bog area.

Site 4 was located in the hummocks area overgrown by *M. gale*; site 3 and site 2 were located in the open bog area with site 2 being further away from "Luther Lake" reservoir than site 3; site 1 was located in the treed bog area. At site 4, shrubs were
20 the dominant PFT, site 3 and 2 had a mixture of PFTs including *Sphagnum* mosses and aerenchymatous graminoids as dominant PFTs. Site 1 accommodated a mixture of PFTs, including *Sphagnum* mosses, trees, graminoid species as well as shrubs. See Table 1 for a summary of the site characteristics and see Fig. S1 for photos of the sites. As indicated from altered stochiometric element ratios (Table 1) and as reported recently by Berger et al. (submitted for publication), those sites in closer proximity to the Luther Lake reservoir are affected by input of nutrients, such as N, P, K, S, Ca, Mg. This translated
25 into a relative enrichment of N, Mg and K and very pronounced P and Ca limitation closer to the reservoir. Moreover, thicker layers of readily decomposable fibric and hemic peat were found up to a depth of approx. 48 cm at sites 1 and 2 whereas at site 3 and 4, strongly decomposed sapric peat was already found below depths of 37 cm (site 3) and 29 cm (site 4) respectively.

All measurements were taken and all samples were collected in hollows.

30 **2.2 Determination of organic matter quality of peat and pore-water**

Bulk peat samples were taken on July 25th, 2014, in depths of 5, 10 and 20 cm below the living *Sphagnum* layer by manual cutting. Peat from 75 cm depth was taken with a Russian peat corer. Peat was filled in jars avoiding any headspace and closed air-tight to maintain anoxic conditions as far as possible during transport to the laboratory.

To collect in-situ pore-water samples, suction samplers (Macro Rhizons, Eijkelkamp, Giesbeck, The Netherlands) with a pore size of about 0.2 μm were inserted into the peat at 5, 10 and 20 cm depth on July 3rd, 2014. Sampling was done by applying vacuum and collecting water with syringes. During sampling, syringes were covered with aluminum foil and peat to avoid exposure to light. Pore-water from 75 cm depth was pumped from 75 cm deep piezometers that were emptied one

5   day prior to sampling to ensure sampling of fresh pore-water. Samples from piezometers were filtered using Macro Rhizons in the laboratory to ensure similar treatment of pore-water of all depths.

All samples were taken and analyzed as three replicates.

Prior to FTIR analysis, oven-dried (70 ° C) bulk peat samples were ground with a ball mill. For pore-water samples 2 mg of oven-dried (70 ° C) organic matter were ground in a mortar with 200 mg of potassium bromide (KBr) and pressed to pellets

10   for analysis. We recorded spectra on an IR-FT-IR Spectrometer (Varian 660, Palo Alto, USA) over a scan range of 4000 to 650 cm^{-1} with a resolution of 2 cm^{-1} and 32 scans per sample. A KBr background was subtracted from the spectra and spectra were baseline corrected. We identified spectral peaks (average location +/- 30 cm^{-1}) and related them to functional moieties as described in Niemeyer et al. (1992). As absorbance values do not give quantitative information on absolute values of functional groups, we related peaks of around 1620 cm^{-1} to 1610 cm^{-1} (aromatic C=C compounds/aromatic moieties) to

15   polysaccharide peaks at 1170 cm^{-1} to 950 cm^{-1} wavenumbers (Niemeyer et al., 1992). A relative increase in ratios thus indicates a relative decrease in the labile polysaccharide moieties and thus a decrease in organic matter quality in regard of a residual enrichment of refractory aromatics (Broder et al., 2012).

Aqueous in-situ pore-water samples were analyzed with a UV-VIS spectrometer (Varian UV 1006 M005 Palo Alto, USA). We recorded UV-vis spectra over a range of 200 to 800 nm with a resolution of 0.5 nm using a 1 cm quartz cuvette. Prior to

20   measurement, the spectrum of a blank with MilliQ-water was recorded and subtracted from each sample. We additionally recorded fluorescence properties of pore-water organic matter on a fluorescence spectrometer (Varian Cary Eclipse, Palo Alto, USA) at a scan rate of 600 nm/min. Excitation wavelengths (ex) were 240 to 450 nm in 5 nm steps, emission wavelengths (em) 300 to 600 nm in 2 nm steps to obtain excitation-emission-matrices (EEMs). If necessary, UV-vis absorption at 254 nm was adjusted to a range of 0.1 to 0.3 by dilution with MilliQ- water to minimize inner filter effects for

25   fluorescence spectroscopy. Repeated blanks with MilliQ-water were run to guarantee cleanliness of the cuvette. Raman spectra of a blank were recorded each day to check analytical drift and to normalize fluorescence to Raman units (Murphy et al., 2010).

To evaluate dissolved organic matter (DOM) quality, we calculated commonly used indices, such as specific ultraviolet absorbance SUVA$_{254}$ (as a proxy for aromaticity, Weishaar et al., 2003) and the E2:E3 ratio (the ratio of UV absorbance at

30   250 nm divided by absorbance at 365 nm) providing information about molecular weight of organic matter (Peuravouri and Pihlaja, 1997) from UV-vis data. From fluorescence data, we calculated a humification index HIX (Ohno, 2002). (see Table S3 for formulas used).)

2.3 Measurements of environmental variables

Air temperature and photosynthetically active radiation (PAR) were recorded about 1 km south of site 1 in an open area by a HOBO U30 weather station (U30-NRC-SYS-B, Onset, Bourne, MA, USA) at a temporal resolution of 5 min. Water table depth below surface (wtd), water temperature (T_{water}) and air pressure were measured using one Solinst Levelogger Edge at

5   each site and one Barologger Gold at site 2 (Solinst Ltd., Georgetown, Canada) in 30-min intervals. On each day of closed chamber measurements, an extra PAR sensor (Smart Sensor, Onset; Part # S-LIA-M003) and an extra temperature sensor (Temperature Smart Sensor, Onset; Part # S-TMB-M0XX) recorded PAR and air temperature at a temporal resolution of 10 secs at the site were chamber measurements were being taken.

2.4 Determination of CO_2 and CH_4 fluxes

10   In the hollows of sites 1-4 a set of six collars for chamber measurements were established in April 2012. The collars - installed 0.1-0.15 m into the soil- were cylindrical, had a diameter of 0.4 m and a total height of 0.2 m. Through object based image analysis (OBIA), the spatial coverages of PFTs at each site were obtained (data summarized in Table 1). Accordingly, the locations for chamber measurement collars of our study sites were defined to proportionally reflect the distribution of PFTs. To preserve the soil and plant structure, and to avoid any bias in gas fluxes during the chamber placement, boardwalks

15   were installed.

Closed chamber measurements were performed following Burger et al., (2016), who employed a similar approach in floating chamber measurements on a nearby pond. Measurements were taken every 10 to 30 days at each site from April, 20th 2014 through September 22nd, 2015. In total 19 to 23 daily courses per site could be accomplished. Two cylindrical Plexiglas chambers were used for the flux measurements: a transparent chamber was used to measure net ecosystem exchange (NEE)

20   while ecosystem respiration (R_{eco}) was measured with a chamber covered with reflective insolation foil. Chamber closure time was 180 secs.

Air was circulated between the chamber and a trace gas analyzer (Ultraportable Greenhouse Gas Analyzer 915-001, Los Gatos Research Inc., Mountain View, USA) through 2 mm inner diameter polyethylene tubing, recording trace gas concentrations of CO_2 and CH_4 at a temporal resolution of 1 sec. According to the manufacturer, the reproducibility of CH_4

25   and CO_2 is < 2 ppb and < 300 ppb, respectively. The analyzer was factory-calibrated immediately before the campaign. Stability of the calibration was checked repeatedly during summer of 2014. In January and July 2015, the analyzer was again re-calibrated. If CH_4 concentrations increased sharply within the first 60 secs of the measurement due to CH_4 bubble release caused by the positioning of the chamber, the measurement was discarded and repeated.

During each measurement day, each collar was monitored several times with the transparent and dark chamber at different

30   times (typically between 5 am and 8 pm) and different PAR levels (typically 5 to 2000 µmol m^{-2} s^{-1}) throughout the day. Unfortunately, due to the remoteness of our study site, measurements at night were not possible.

Gas fluxes were determined by Eq. 1:

$$F_{chamber} = \frac{\Delta c}{\Delta t \, A} \cdot \frac{P \, V}{R \, T},$$

5   based on the changes of concentration over time inside the chamber, applying the ideal gas law with the ideal gas constant R,
and correcting for atmospheric pressure P and temperature inside the chamber T. The chamber volume V and basal area A
were calculated from the chamber's physical dimensions, taking into account each collar's vegetation volume, determined in
May, July and October 2014 as well as in April and August 2015 and extrapolated for the other campaigns. The
concentration change over time was derived from the slope of a linear regression of concentration vs. time. The first 40 secs

10 after chamber deployment were discarded to account for the analyzer's response time. If the slope was not significantly
different from 0 (tested with an F-test, $\alpha = 0.05$), the flux was set to zero.

An empirical description of the measured NEE fluxes of each site was accomplished with the help of a hyperbolic light
response model (Owen et al., 2007). The non-linear least squares fit of the data to the model was done according to Eq. 2:

15 $$NEE = \frac{\alpha \beta Q}{\alpha \beta} + y$$

where NEE is in mol m^{-2} s^{-1}, α is the initial slope of the light response curve (in mol CO$_2$ m^{-2} s^{-1} per mol photon m^{-2} s^{-1}), β is
the maximum NEE in mol CO$_2$ m^{-2} s^{-1}, Q is the photosynthetic active radiation in mol photon m^{-2} s^{-1}, and γ is an estimate of
the average R_{eco}. Integration of NEE over the course of one day gave net daily ecosystem production (NEP). Gross primary

20 productivity (GPP) was retrieved by subtracting R_{eco} from NEP.

Average CH$_4$ fluxes of measurement days of each site were obtained and lastly, cumulative emissions of CO$_2$ and CH$_4$ were
calculated likewise according to Tilsner et al. (2003).

To determine isotopic signatures of CH$_4$ fluxes, we carried out additional chamber flux measurements once a month from
May to September 2015 using a shrouded chamber and the Los Gatos UGGA. The chamber was closed until CH$_4$

25 concentrations inside were high enough for analysis of isotopic composition (at least 10 ppm), but not more than 30 min.
Samples for isotopic analysis were extracted from the chamber with 60 ml syringes through a polyethylene tube with a three-
way stopcock on one end and filled into 40 ml crimp vials that had before been flushed with nitrogen (N$_2$) and sealed with
rubber stoppers. To correct isotopic values of CH$_4$ for background isotopic signature in the chamber, we collected six air
samples at each site on every sampling day. Analysis was carried out as outlined for dissolved gases (see below).

2.5 Temporal dynamics of CO_2 and CH_4 concentrations and $\delta^{13}C$-CO_2 and $\delta^{13}C$-CH_4-values along peat pore-water profiles

2.5.1 Sampling of gases and dissolved gases in the peat

Concentrations of CH_4 and dissolved inorganic carbon (DIC/ΣCO_2) along peat profiles were analyzed in 5, 15, 25, 35, 45

5   and 55 cm depth with three replicates at each site using diffusive equilibration samplers made of permeable silicon tubes (Kammann et al. 2001). Through a three-way stopcock, samples were taken with 10 ml syringes every two to three weeks, starting on June 16th, 2014, ending on September 22nd, 2015. Samples were stored in a refrigerator overnight at 5 ° C and analyzed for concentrations the next day.

   To determine temporal dynamics of isotopic signatures of CH_4 and CO_2 in the peat, we installed a separate set of silicon

10 tubes in 5, 15, 25 and 35 cm depth with three replicates each per site. These latter silicon tubes had an inner diameter of 0.5 or 1 cm and a volume of 20 ml in 5 cm depth and 5 ml in the other depths, in order to obtain a sample volume of at least 20 ml at sufficiently high concentration ($2.5 < x < 2000$ ppm) for isotope analysis. Samples were taken once a month from May 2015 to September 2015 with 10 and 60 ml syringes and filled in 10 respectively 40 ml crimp vials that were before flushed with N_2 and sealed with rubber stoppers. Silicon samplers were refilled with N_2 to avoid oxygen entering the system.

15 All samplers were installed one month prior to the first sampling to assure equilibration, and tightness of all samplers was confirmed prior to installation.

   To obtain high resolution depth profiles of concentration and isotopic signatures of CH_4 and DIC, pore-water peepers of 60 cm length and a 1 cm resolution (Hesslein 1976) were inserted on three occasions in June, July and September 2015 and allowed to equilibrate for four weeks prior to sampling. As results of pore-water peepers generally confirmed the data of the

20 silicon samplers, results are not presented here but described in the supporting information (see Fig. S6).

2.5.2 Analyses of CO_2 and CH_4 concentrations and $\delta^{13}C$-CO_2 and $\delta^{13}C$-CH_4-values

Gaseous CO_2 and CH_4 concentrations were analyzed with a gas chromatograph (SRI 8610 C, SRI Instruments, Torrance, US) equipped with a Flame Ionization Detector (FID) and a Methanizer. Samples from pore-water peepers were analyzed by measuring the headspace concentration in the vials.

25 Rations of $\delta^{13}C$ of CO_2 and CH_4 were determined by Cavity Ringdown Spectroscopy (CRDS; Picarro G2201-*i*, Picarro Inc., Santa Clara, US), simultaneously determining ^{13}C isotopic composition of CO_2 and CH_4 with a precision of <0.16 ‰ for $\delta^{13}C$-CO_2 and <1.15 ‰ for $\delta^{13}C$-CH_4. The Analyzer was calibrated before every measurement with two working standards of CO_2 (1000 ppm, -31.07 ‰) and CH_4 (1000 ppm, -42.48 ‰). Standard deviation for $\delta^{13}C$-CO_2 was below 2 ‰ and below 4 ‰ for $\delta^{13}C$-CH_4. Isotopic signatures were expressed in the δ-notation in ‰ versus VPDB-Standard according to Eq. 3:

$\delta^{13}C = (R_{sample}/R_{standard} - 1) \cdot 1000 \ [‰]$

where R_{Sample} is the $^{13}C/^{12}C$ ratio of the sample and $R_{Standard}$ is the $^{13}C/^{12}C$ ratio of the standard.

As the accuracy of $\delta^{13}C$-CO_2 values was affected by high CH_4 concentrations present in the samples, we established a correction formula to revise $\delta^{13}C$-CO_2 values. This formula was applied for concentration ratios of $CO_2:CH_4$ between 0.3 and 1.5. Samples with $CO_2:CH_4$ ratios < 0.3 could not be corrected and were discarded; samples with higher ratios did not need

5 correction. To cross-check values of $\delta^{13}C$-CO_2, two additional standards, carbonic acid from fermentation (-26.61 ‰), natural carbonic acid (-0.19 ‰) and a mixture of both (-15.16 ‰) were measured both with CRDS and an isotope-ratio mass spectrometer (EA/TC-IRMS Nu Horizon, Hekatech/Nu Instruments, Wrexham, UK). Additionally, $\delta^{13}C$-CO_2 values had to be corrected for a storage effect. As samples were stored for several weeks, CO_2 was lost from the vials and isotopic signatures increased by 0.056 ‰ per day. There was no such effect detectable for CH_4.

10 Dissolved concentration of CO_2 and CH_4 were recalculated from partial pressures inside the silicon samplers applying Henry's Law according to Eq. 4:

$$c = K_H * p$$

15 where c is the concentration in µmol/L, p is the pressure in atm and K_H is the in-situ temperature corrected Henry-constant in mol L^{-1} atm^{-1} (Sander, 1999). CO_2 dissociation was considered using equilibrium constants from Stumm and Morgan (1996) to calculate the total amount of DIC.

DIC and CH_4 concentrations in samples from pore-water peepers were recalculated from gas concentrations in the headspace, applying the ideal gas law and temperature corrected Henry-constants for laboratory conditions.

20 **2.6 Statistical analysis**

Statistics software R i386 version 3.1.0 was used to verify if observed differences in organic matter quality varied between depths and sites were statistically relevant for each indicator separately. Data was tested for normal distribution (Shapiro-Wilk-Test, α = 0.05) and homogeneity of variance (Levene-Test, α = 0.05). In case both requirements were met, we carried out a one-way ANOVA (Analysis of Variance) (α = 0.05) with a post-hoc Tukey's Honest Significant Difference (HSD) test

25 (α =0.05) to identify which depths or which sites differed significantly. If either normal distribution or homogeneity of variance were not given, a Kruskal-Wallis test (α = 0.05) with a multiple comparison test after Kruskal-Wallis (α = 0.05) as post-hoc test was executed.

Using *RStudio* Version 0.99.902 as well as R i386 3.2.3 we examined whether there were significant differences in $\delta^{13}C$ values of CO_2 and CH_4, CO_2 and CH_4 concentrations and cumulative emissions between the sites. Means were compared

30 with t-Tests (normally distributed data) respectively Kruskal-Wallis and post hoc Wilcoxon-Mann-Whitney-Test (data not normally distributed) at a confidence level of α = 0.05. Normality was tested with Shapiro-Wilk-Test (α = 0.05) and homogeneity of variance was confirmed with Levene-Test (α = 0.05). Correlations between environmental variables and fluxes, concentrations and isotopic signatures were determined with Pearson's product-moment correlation for normally

distributed data or with Spearman's rank correlation if data was not normally distributed. With ANOVA ($\alpha = 0.05$), the effect of categorical variables on CH_4 fluxes and $\delta^{13}C$ values was computed.

3 Results

3.1 Organic matter quality of peat and pore-water

5   The highest degree of bulk peat decomposition, as indicated by the highest 1618.5/1033.5 ratios, was found at site 4 between 5 and 20 cm depth ($p < 0.05$ in 10 and 20 cm depth), indicating the highest degree of bulk peat decomposition at this site and these depths (Fig 2 (a)). The 1618.5/1033.5 ratios of the sites 1-3 were not significantly different.

Pore-water samples´ 1618.5/1033.5 ratios of site 3 were smallest between 5 and 20 cm depth as compared to all other sites ($p < 0.05$), indicating the lowest degree of decomposition of DOM (Fig 2 (b)).

10 Aromaticity as determined with $SUVA_{254}$ (Fig 2 (c)) did not show significant differences between sites in pore-water samples (exception: site 1 and site 3 in 20 cm depth ($p = 0.033$), where site 1 $SUVA_{254}$ was significantly higher than site 3 $SUVA_{254}$). Site 3 had the lowest aromaticity at the upper layers (5 cm to 20 cm depth), however, the difference was not statistically significant.

The degree of humification, as depicted by HIX (Fig 2 (d)), was significantly lowest in site 3 pore-water (5 cm site 3 and 4: p

15 $= 0.026$; 10 cm site 1 and 3: $p = 0.014$; 20 cm site 3 and 4: $p = 0.020$).

The slope ratio $E2:E3$ (Fig 2 (e)), indicative of molecular size and aromaticity, indicated decreasing aromaticity and decreasing molecular weight in the order of site 4 > site 1 > site 2 > site 3.

3.2 Development of wtd and T_{water} during the study period

During our study period, hollow wtd showed strong seasonal fluctuations; maximum wtd (i.e. highest water table levels)

20 throughout the study period were reached during snowmelt in spring 2014 (site 1: 6.94 cm, site 2: 4.99 cm, site 3: 16.26 cm, site 4: 23.18 cm above surface), minimum wtd (i.e. lowest water table levels) were reached during the summer of 2015 (site 1: 32.5 cm, site 2: 31.75 cm, site 3: 13.34, site 4: 19.11 cm below surface). The sites 1 to 4 all showed similar courses of wtd, however, at site 3 and site 4 water levels were generally higher as compared to site 1 and 2. The range between maximum and minimum wtd at all sites was overall similar (site 1: ~39.5 cm, site 2: ~36.7 cm, site 3: ~30 cm (logger failure when

25 water levels were lowest), site 4: ~42.3 cm). T_{water} varied between ~2 °C in winter and ~16 °C in summer. Detailed courses of wtd and T_{water} are presented in the top panels of the figures 3 and 4.

3.3 Fluxes of CO_2 and CH_4 at the soil/atmosphere interface, concentrations of CH_4 and DIC along soil profiles during the study period

DIC concentrations (Fig. 3 and 4) varied strongly throughout the year. Maximum DIC concentrations were observed below

30 20 cm depth in autumn 2014 and winter 2014/2015 and minimum concentrations were observed during snowmelt in March

and April 2015. DIC concentrations at site 4 at all depths were overall lower and significantly decreased ($p < 0.05$) in comparison to all other sites from February 23rd through April 4th, 2015; moreover, site 4 DIC concentrations were significantly ($p < 0.05$) lower than site 3 DIC concentrations on August 6th, 2014 and between April 19th through July 18th, 2015.

5 A similar pattern was observed for CH_4 concentrations (Fig. 3 and 4), as they were increasing during the growing season, reached maximum values in the winter season 2014/2015 and comparably decreased during snowmelt in spring. Concentrations in the uppermost depths of both CO_2 and CH_4 were strongly affected by wtd fluctuations, with strong decreases upon water table decline and vice versa.

Fluxes of CO_2 and CH_4 (Fig. 3 and 4) showed a strong annual variability. Overall, NEP, GPP, and R_{eco} at all sites were
10 highest during the growing seasons. Also, CH_4 fluxes were highest during the growing season, despite comparably low concentrations of dissolved CH_4 in the investigated upper 50 cm of the peat profile, suggesting that exchange of gases at the peat/atmosphere interface and concentrations in the uppermost peat were decoupled.

Accordingly, NEP, GPP, R_{eco} and CH_4 fluxes at almost all sites were positively correlated with T_{water} ($p < 0.05$), however, negatively correlated with wtd (lowest water tables co-occurred with highest fluxes). As suggested from visual inspection,
15 R_{eco}, GPP and CH_4 fluxes of the sites 1, 2 and 3 were in most cases negatively correlated with DIC and CH_4 concentrations along soil profiles, i.e. increasing CO_2 and CH_4 fluxes were correlated with decreasing DIC and CH_4 concentrations. Only at site 4 greater DIC and CO_2 concentrations along peat profiles coincided with higher effluxes of CO_2 and CH_4. Statistical results are summarized in the Table S4.

During the study period, hollows of site 1 accumulated 1552 ± 652 g CO_2 m^{-2} and released 41.8 ± 25.4 g CH_4 m^{-2}, site 2
20 accumulated 1637 ± 184 g CO_2 m^{-2} and released 44.6 ± 13.7 g CH_4 m^{-2}, site 3 accumulated 2260 ± 480 g CO_2 m^{-2} and released 61.4 ± 32 g CH_4 m^{-2} and site 4 accumulated 1093 ± 794 g CO_2 m^{-2} and released 46.1 ± 35.2 g CH_4 m^{-2} (see Fig. S5). Between May 19th, 2014 and September 23rd, 2015 site 4 accumulated significantly less CO_2 as compared with the other three sites ($p < 0.001$), while there were no statistically significant differences in terms of CO_2 uptake for the sites 1, 2 and 3. Moreover, site 3 emitted significantly more CH_4 as compared with the sites 1, 2 and 4 ($p < 0.001$).

25 **3.4 Temporal and spatial variability of δ^{13}C-CO_2 and δ^{13}C-CH_4 -values in peat pore-gas profiles during the growing season in 2015**

Values of δ^{13}C of the sampled CH_4 in the peat ranged from -78.74 to -26.77 ‰, δ^{13}C signatures of CO_2 ranged from -25.81 to +4.03 ‰ (see Fig. 5). Highest δ^{13}C-CH_4 and CO_2 values were measured at site 1 in 5 respectively 35 cm depth in September. Lowest δ^{13}C-CH_4 and CO_2 values were detected at site 1 in 15 cm depth in June and at site 2 in 15 cm depth in
30 August respectively.

Overall, δ^{13}C-CH_4 values showed an increasing trend with time from June to August in all depths. Average signatures in 5 to 35 cm depth differed significantly between sampling dates at all sites except between August and September ($p < 0.05$).

Concomitant to a decline in water tables in August and September, δ^{13}C-CH$_4$ signatures shifted to less negative values in the upper 5 cm at sites 1 to 3; this shift was most distinctive at site 1 and least distinctive at site 3. At site 4, such shift occurred at 15 cm depth.

For δ^{13}C-CO$_2$ signatures, significant differences between some sampling dates were found at sites 1, 2 and 4 for average values in 5 to 35 cm depth. At sites 1 and 2, signatures in August and September were higher than in June and July, paralleling the trend in δ^{13}C-CH$_4$. At site 3 and 4, such significant shifts could not be observed.

No significant differences between depths could be found for either δ^{13}C-CH$_4$ or δ^{13}C-CO$_2$ signatures at any site. Anyway, at sites 1 and 2, δ^{13}C-CH$_4$ signatures apparently increased with depth in June and July, no trend was observable at sites 3 and 4. In August and September, δ^{13}C-CH$_4$ signatures seemed to decrease with depth except for site 4. Values of δ^{13}C of CO$_2$ increased with depth except at site 1 in July and at site 2 in July and August.

Mean signatures of δ^{13}C-CH$_4$ at site 4 (-57.81 ±7.03 ‰) differed significantly from those at the other sites (site 1: -61.48 ±10.71 ‰, site 2: -60.28 ±5.57 ‰, site 3: -62.30 ±5.54 ‰) for the whole sampling period ($p < 0.01$, $p < 0.05$, $p < 0.001$).

δ^{13}C-CO$_2$ signatures at site 3 were significantly higher than at the other sites in July ($p < 0.05$, $p < 0.01$, $p < 0.01$). Overall, highest mean values were found at site 1 (-12.05 ± 8.23 ‰) whereas site 4 revealed lowest δ^{13}C-CO$_2$ signatures (-15.85 ± 3.61 ‰).

3.5 δ^{13}C signatures of emitted CH$_4$ during summer 2015

δ^{13}C signatures of CH$_4$ fluxes lay between -81.87 ± 3.81 and -55.61 ± 1.20 ‰ (see Fig. 6). Lowest δ^{13}C values were measured in May at site 3 (Fig. 6 (c)). Highest values were observed in August at site 2 (Fig. 6 (b)).

δ^{13}C- CH$_4$ signatures were increasing from July to August and slightly decreased in September. Significant differences were only found at sites 3 and 4 between July and August ($p < 0.01$, $p < 0.05$), however, from visual inspection of the panels (a) – (d) of Fig. 6 δ^{13}C- CH$_4$ values seemed to increase between May and September at site 3, while they appeared to decrease at site 4, with very distinct values in August. There was no such development observable at the sites 1 and 2. Summing up δ^{13}C- CH$_4$ signatures from all sites, isotopic signatures in July differed significantly from those in August and September ($p < 0.05$). In September, isotopic signatures of the CH$_4$ flux at site 2 differed significantly from those at the other sites ($p < 0.05$).

The distinct patterns of August may have to be interpreted with caution due to limitations in our sampling technique, in particular when water tables were lowest (see discussion Sect. 4.3).

Plant mediated transport was the dominant CH$_4$ emission pathway during the summer 2015 at all sites and all sampling dates according to Hornibrook (2009) (Fig. 6 (e)).

4 Discussion

Along our studied gradient of four sites it became evident that the peatland was exposed to nutrient infiltration from the water reservoir and thus elevated nutrient concentrations occurred in vicinity to the water reservoir, as reported elsewhere (Berger et al., submitted for publication). This was clearly visible in C/N, C/Mg and C/K ratios, decreasing in the order of

5 site 4 < 3 < 2 < 1, while C/P, N/P and C/Ca ratios increased in vicinity to the reservoir, indicating a limitation of P and Ca, which is typical of eutrophic peatlands (see Berger et al., submitted for publication and Table 1). Moreover, pronounced differences in terms of vegetation were evident: While at site 4 the predominant PFT were shrubs and *Sphagnum* mosses were in retreat, sites 2 and 3 were dominated by a mixture of *Sphagnum* mosses and graminoids, and site 1 accommodated a mixture of PFTs, such as *Sphagnum* mosses, graminoids, dwarf shrubs and few trees. In addition to those characteristics,

10 further differences in terms of water table regimes were observed, i.e. sites 3 and 4 were apparently wetter than sites 1 and 2. Moreover, there were pronounced differences in gas fluxes and peat quality, while the dominant CH_4 emission pathway was plant-mediated transport at any site. An interpretation of the interplay of processes, fluxes, and vegetation based on our results will be discussed in the following.

4.1 Peat quality

15 The FTIR ratio derived peat quality index revealed the highest degree of bulk peat decomposition in the upper peat layers of shrub dominated site 4 (Fig 2 (a)), while there were no significant differences in bulk peat decomposition degree as far as the other sites were concerned. On the other hand, in the upper depths of graminoid-moss dominated site 3, pore-water DOM quality indicators mostly revealed a significantly lower share of aromatic compounds, fewer humic substances, a lower degree of humification and comparably increased molecular weight at that site (Fig 2 (c)-(e)). This more labile nature of

20 dissolved organic matter compared to otherwise similar bulk peat quality suggested some inflow of water and solutes, presumably from the reservoir, delivering labile matter to fuel decomposition.

This result partly corroborates our hypothesis 1, that in closer vicinity to the reservoir, where nutrient input is greatest, C-cycling is accelerated as indicated by more decomposed bulk peat.

Indeed, site 4, which also had the highest abundance of the PFT of shrubs, featured a significantly increased degree of

25 decomposition, indicating an accelerated C-cycle. This higher degree of decomposition may however be also explained by the presence of shrubs, rather than by the close vicinity to the reservoir, because sites 1-3 did not show any significant differences in their degree of bulk peat decomposition but significantly lower coverage of shrubs. Shrubs contain more woody parts and thus have higher lignin contents and more phenolic groups than graminoids or mosses and they are also more productive than mosses and graminoids (Bragazza et al., 2007). In recent studies, an increasing ericaceous shrub cover

30 was associated with increasing polyphenol content in plant litter and pore-water, as well as increasing phenol oxidase in litter of ericaceous shrubs. Also, a higher release of labile C from vascular plant roots was observed. These changes, however along an altitudinal gradient, were accompanied by a decreasing *Sphagnum* productivity (Bragazza et al., 2013; Bragazza et

al., 2015). Even though at site 4 we primarily dealt with eutrophication, rather than warming, there might be similar processes explaining our observations: Shrubs outcompete *Sphagnum* mosses after long term-nutrient infiltration and a reduced recalcitrance of the peat arising from shrub litter may result in a reduced C assimilation, i.e. peat accumulation (Turetsky et al., 2012; Larmola et al., 2013; Ward et al., 2013). This was further suggested by the lowest CO_2 uptake and

5 lowest DIC concentrations along peat pore-gas profiles throughout the study period at that particular site.

FTIR ratios of our study compare well with other studies (e.g. Blodau and Siems, 2010; Biester et al., 2014), as well as ranges of UV-vis and fluorescence spectroscopy based indices (see Table S7). The degree of humification (HIX) was high at Wylde Lake peatland complex but not as high as at poorly drained thermokarst wetland sites, moderately well drained and well drained sites in central Alaska, USA (Wickland et al., 2007).

10 **4.2 Seasonal development of water table regimes and carbon fluxes**

Water tables and water temperatures followed a clear seasonal pattern. During the growing seasons, water tables notably dropped and temperatures increased as expected, while during the winter season and snowmelt period water levels were highest and temperatures were lowest. Among the four sites, water levels tended to be on average higher towards the shoreline of the water reservoir (sites 3 and 4). The hollows of these sites thus do not only reflect conditions of elevated

15 nutrient supply, but also on average wetter conditions.

As observed for wtd and T_{water}, NEP, R_{eco}, GPP and CH_4 fluxes followed seasonal patterns as well (see Fig. 3 and 4). Over the entire study period (April 2014 through September 2015) cumulative NEP increased in the order of site 4 < 1 < 2 < 3, meaning that the two graminoid dominated sites accumulated the highest amount of CO_2, in the case of site 3 this was also statistically significant. In contradiction to the first part of our hypothesis 2 (greatest CO_2 uptake at the shrub dominated and

20 mostly fertilized site) our wet and shrub dominated site 4 showed the lowest cumulative CO_2 uptake. In previous studies, a greatest decrease in the CO_2 sink-strength was observed when graminoids were dominant (Larmola et al., 2013; Ward et al., 2013; Kuiper et al., 2014), while in our study site 3, where *Sphagnum* mosses and graminoids were the dominant PFT and where wtd was comparable to shrub dominated site 4, the highest CO_2 uptake was observed. Moreover, the CO_2 uptake rates of all our sites exceeded reported CO_2 uptake rates of bogs by far, irrespective of predominant PFTs, and were comparable to

25 uptake rates reported for fens (Lund et al., 2010), which can be well related to increased nutrient availability as discussed in Berger et al., (submitted for publication).

Partitioning of NEP into R_{eco} and GPP illustrated the observed differences in CO_2 fluxes between sites. Our wet and graminoid-moss dominated site 3 reached great rates in GPP of up to -26.65 g CO_2 m^{-2} d^{-1}, while R_{eco} never exceed rates of 22.07 g CO_2 m^{-2} d^{-1}. The maximum GPP of the comparably drier, graminoid-moss dominated site 2 (-19.79 g CO_2 m^{-2} d^{-1})

30 also remained well above maximum R_{eco} here (15.49 g CO_2 m^{-2} d^{-1}). In contrast, R_{eco} of site 1 with a mixture of PFTs but comparably dry, as well as of wet and shrub dominated site 4 reached up to 31.56 g CO_2 m^{-2} d^{-1} while GPP remained comparable to sites 2 and 3 (maximum CO_2 uptake rates of -24.22 g CO_2 m^{-2} d^{-1}). Thus, rather an increase in R_{eco} than a decrease in GPP, accounted for the differences in NEP between our study sites.

Cumulative CH_4 release increased in the order of site 1 < 2 < 4 < 3, partly confirming that graminoid sites show highest CH_4 emission (hypothesis 2). In existing studies, greatest emissions were typically found in wetter habitats dominated by graminoids (Levy et al., 2012, Gray et al. 2013).

Interestingly, in our study NEP, GPP and CH_4 emissions were negatively correlated with CH_4 and DIC concentrations in the
5 uppermost 50 cm of the profiles at the sites 1, 2 and 3. The sites 2 and 3 were predominated by a greater share of graminoids, while all the sites 1, 2 and 3 appeared to accommodate a healthy *Sphagnum* moss community and a bog typical vegetation, even though our mixture of PFTs site 1 featured comparably less graminoids. Such a decoupling of CO_2 and CH_4 fluxes from pools in the peat was already observed in previous studies: Graminoids are known to be important facilitators of CH_4 emissions because they can transport CH_4 from water-saturated layers of the peat into the atmosphere via aerenchyma and
10 bypass the zone of CH_4 oxidation (Shannon and White, 1994; Marushchak et al., 2016). Moreover, they supply exudates via their roots, stimulating microbial activity and accordingly methanogenesis (Bubier et al., 1995). Through their deeper rooting system, graminoids may thus have connected the CH_4 pools of deeper layers below our studied profile, i.e. below 50 cm depth, to fuel the observed surface fluxes. The decreasing concentrations of CH_4 in surface near layers due to a decrease in water table levels and partial aeration did thus not translate in lower fluxes as suggested by Strack et al. (2006). Also, at low
15 water tables and unsaturated conditions higher diffusivity for CO_2 can occur, leading to notably higher diffusive fluxes despite low concentrations (Knorr et al., 2008). It is striking that DIC concentrations at the wet and shrub dominated site 4 were notably lower as compared with other sites. A reasonable explanation is a lower peat quality resulting from deepening of soil oxygenation, stimulating microbial decomposition in the presence of deciduous shrubs (Bragazza et al., 2016), which are being promoted in closer vicinity to the eutrophic water reservoir. Such soil aeration would contradict wetter conditions
20 as would be expected by the water reservoir. However, in close proximity to the reservoir, also an advective redistribution and removal of CO_2 and CH_4 through advective flow cannot be excluded.

4.3 Methane production, methanotrophy and pathways of CH_4 emissions as inferred from stable isotopes

Isotopic composition of CO_2 and CH_4 indicated clear differences between sites and depth (see Fig. 5), corresponding to observed patterns in concentrations and inferred production, consumption, or emissions. In general, δ^{13}C-CH_4 signatures
25 along soil profiles of all sites increased between June and August, i.e. CH_4 got more enriched in ^{13}C, suggesting that CH_4 oxidation must have been an important factor throughout the dry season in summer when the water table notably dropped. Methane oxidation is known to cause more ^{13}C-enriched CH_4 that is even ^{13}C enriched compared to the ambient CH_4 (Alstad and Whiticar, 2011), as was observed here. Our least negative values (-26.77 ‰), observed at 5 cm depth of mixture-of-PFTs site 1, markedly exceeded those found in other studies (e.g. Bellisario et al., 1999; Corbett et al., 2013), which had been
30 conducted in peats subjected to anoxic conditions, where oxidation of CH_4 did not play an important role. Moreover, δ^{13}C-CH_4 signatures at 5 cm depth of different sampling dates appeared to be most variable at the sites 1 and 2, which were also found to be drier than the sites 3 and 4, where less pronounced shifts of δ^{13}C-CH_4 signatures occurred throughout the sampling period. Another interesting finding was the strong oxidation signal at 15 cm depth of shrub dominated site 4 in

August 2015 (-39.10 ‰) as compared to -57.73 ‰ in 5 cm depth, which could have to do with more aerated peat due to rooting of shrubs and the deepening of soil oxygenation probably promoting a highly active methanotrophic bacteria community, which drew CH_4 from the atmosphere down to that depth, resulting in a more pronounced CH_4 oxidation signal in 15 cm than in 5 cm depth. The shrub dominated site 4 also featured the most enriched δ^{13}C-CH_4 signatures in general,

5   suggesting either, least CH_4 production or most CH_4 oxidation here. The wet and graminoid-moss dominated site 3, showed the smallest variations in δ^{13}C-CH_4 signatures throughout the sampling period, suggesting least modification of δ^{13}C-CH_4 from oxidation here, which corresponds well with greatest CH_4 emissions measured at that site.

Our δ^{13}C-CO_2 values ranging from -25.81 to + 4.03 ‰ also agreed well with other studies (e.g. Landsdown et al., 1992; Hornibrook et al., 2000), although comparably less data on ^{13}C in CO_2 from other studies is available. Overall lowest values

10   were found at shrub dominated site 4, suggesting a higher share of CO_2 from increased CH_4 oxidation. High CO_2 emission despite strikingly low DIC concentrations, which we observed along the site 4 peat profiles during the entire study period, suggest that the CO_2 stemmed from increased respiration through stronger aeration and parallel CH_4 oxidation in the site 4 peat. Our δ^{13}C-CO_2 values generally got more enriched in ^{13}C with depth at all sites and sampling dates, as expected from ongoing methanogenesis. Great shifts in δ^{13}C-CO_2 values of the drier sites 1 and 2 during the entire sampling period could

15   again be explained by penetrating atmospheric CO_2 with dropping water tables in August. Moreover, according to Hornibrook et al. (2007), methanogenesis in semi-terrestrial environments typically leads to δ^{13}C-CO_2 values between -20 and -5 ‰ if dominated by an input of C3 vegetation, which is the case in the Wylde Lake peatland complex.

Regarding isotopic signatures of the emitted CH_4, in general, the emitted CH_4 (see Fig. 6 (a) – (d)) was lighter than the CH_4 in the pore-gas (see Fig. 5) of the upper peat layers, suggesting that the emitted CH_4 must have been produced in the deeper

20   peat layers (Marushchak et al., 2016). Here, δ^{13}C-CH_4 signatures were more depleted and during transport through plant aerenchyma, the lighter CH_4 could bypass oxidation. Interestingly, plant mediated transport was the dominant CH_4 emission pathway even at the shrub dominated site 4 and mixture-of-PFTs site 1, where graminoid cover accounted only for about 10 %. So, our assumption that the dominant CH_4 emission pathway is plant-dominated transport where aerenchymatous graminoids are abundant while the shrub dominated site features mostly CH_4 diffusion (hypothesis 3) is to be rejected. Plant-

25   mediated transport was the dominant CH_4 emission pathway at all sites and at all sampling dates. We suggest that this is due to the great CH_4 oxidation in the upper peat layers and rather high concentrations at greater depth, facilitating plant mediated transport and ebullition. As already mentioned in the results Sect. (3.5) we would prefer to not overinterpret the variation in δ^{13}C-CH_4 signatures throughout the growing season, because we think that by placing our chambers for isotope sampling when wtd was lowest (in August 2015), we might have pushed additional CH_4, which was subject to oxidation, out of the

30   upper peat layers. However, given the limitations in our sampling technique, the δ^{13}C-CH_4 values of emitted CH_4 were still much lower than the pore-gas δ^{13}C-CH_4 values of the upper peat layers, further underlining that plant-mediated transport was the dominant CH_4 emission pathway. From visual inspection of the panels (a) – (d) of Fig. 6 and Fig. 5 we suggest that the emitted CH_4 originated from at least -25 cm depth or below.

5 Concluding remarks

Our case study shows that certain PFTs co-occurred with pronounced differences in carbon cycling and associated peat quality. A large uptake of CO_2 and a remarkable release of CH_4 in 1.5 years at the graminoid-moss dominated site 3 was accompanied by more degradable and less aromatic pore-water quality. On the contrary, the shrub dominated site 4, which

5 experienced the same water table fluctuations and similar nutrient supply like site 3, featured lowest productivity in terms of CO_2 uptake during the study period, highest degree of bulk peat decomposition and strikingly low DIC concentrations. Two more study sites, of which one had a very similar vegetation cover like site 3 and the other one inhabited a mixture of PFTs, however, being less affected by the nutrient supplying and wtd altering water reservoir, had similar to each other, but different results as compared to the sites 3 and 4.

10 Our results suggest that a graminoid-moss dominated peatland site can withstand eutrophication better than a shrub dominated site (which was also suggested by Wu et al., (2015)). We suggest that there could be a tipping point, when a peatland system shifts from still being productive even though experiencing eutrophic conditions to decreasing productivity, which might co-occur with a spreading of shrub dominated vegetation. If such systems shift to shrub dominated systems, which are exposed to high nutrient deposition even at high water tables, there would be a negative feedback in terms of

15 carbon sequestration.

Our results further suggest that in a eutrophic peatland, which experiences strong water table dropdowns during the growing season, plant mediated transport is the dominant CH_4 emission pathway, even in a shrub dominated site and in mixture of vegetation site, where graminoid cover was only 10 %, because oxidation of CH_4 strongly counteracted CH_4 emission through diffusion.

20 **6 Data availability**

The data can be accessed by email request to the corresponding authors.

Author contributions. Christian Blodau, Klaus-Holger Knorr and Sina Berger designed the experiments, Sina Berger, Leandra Praetzel and Marie Goebel carried them out. Sina Berger prepared the manuscript with contributions from Klaus-

25 Holger Knorr, Leandra Praetzel and Marie Goebel.

The authors declare that they have no conflict of interest.

Acknowledgements. We are grateful for funding by the Deutsche Forschungsgemeinschaft (DFG) (BL563/21-1) We thank

30 Martin Neumann from the Grand River Conservation Authority for the permission to carry out research in the Luther Marsh Wildlife Management Area and we thank Claudia Wagner-Riddle, Peter Smith and Linda Wing for their help on organizational issues. We also thank Inge-Beatrice Biro, Magdalena Burger, Ines Spangenberg, Niclas Kolbe, Eike Esders,

Michael Rammo, Nils Vickus, Fabian Benninghoff, Leonie Fröhlich, Jörg Rostek and Cornelia Mesmer for their support in the field. Analyses of CO_2 and CH_4 concentrations, $\delta^{13}C$ abundance and spectral analyses of various samples were carried out at the institutional lab or the Institute of Landscape Ecology, University of Münster. We thank Stefanie Holm, Ronya Wallis and Madelaine Supper for assistance during analysis of numerous samples in the laboratory.

5 This paper is dedicated to the memory of Christian Blodau, who led the Wylde Lake peatland project until he tragically passed away in July 2016.

References

Alstad, K. P., Whiticar, M. J.: Carbon and hydrogen isotope ratio characterization of methane dynamics for Fluxnet peatland ecosystems, Org Geochem, 42(5), 548–558, 2011.

Berger, S., Gebauer, G., Blodau, C., Knorr, K.-H.: Peatlands in a eutrophic world – assessing the state of a poor fen-bog transition in southern Ontario, Canada, after long term nutrient Input and altered hydrological conditions, under review.

Bellisario, L. M., Bubier, J. L., Moore, T. R.: Controls on CH_4 emissions from a northern peatland, Global Biogeochem
15 Cycles, 13(1), 81–91, 1999.

Biester, H., Knorr, K.-H., Schellekens, J., Basler, A., and Hermanns, Y.-M.: Comparison of different methods to determine the degree of peat decomposition in peat bogs, Biogeosciences, 11, 2691–2707, 2014.

20 Blodau, C.: Carbon cycling in peatlands - A review of processes and controls, Environ Rev, 10, 111–134, 2002.

Blodau, C., Siems, M.: Drainage-induced forest growth alters belowground carbon biogeochemistry in the Mer Bleue bog, Canada, Biogeochemistry, 107, 107–123, 2010.

25 Bragazza, L., Siffi, C., Lacumin, P., Gerdol, R.: Mass loss and nutrient release during litter decay in peatland: The role of microbial adaptability to litter chemistry, Soil Biol Biochem, 39(1), 257–267, 2007.

Bragazza, L., Parisod, J., Buttler, A., Bardgett, R. D.: Biogeochemical plant-soil microbe feedback in response to climate warming in peatlands, Nat Clim Change, 3, 273–277, 2013.

Bragazza, L., Bardgett, R. D., Mitchell, E. A. D., Buttler, A.: Linking soil microbial communities to vascular plant abundance along a climate gradient, New Phytol, 205, 1175–1182, 2015.

Bragazza, L., Buttler, A., Robroek, B., Albrecht, R., Zaccone, C., Jassey, V., Signarbieux, C.: Persistent high temperature and low precipitation reduce peat carbon accumulation, Glob Change Biol, 22, 4114–4123, 2016.

5   Breeuwer, A., Robroek, B. J. M., Limpens, J., Heijmans, M. M. P. D., Schouten, M. G. C., Berendse, F.: Decreased summer water table depth affects peatland vegetation, Basic Appl Ecol, 10, 330–339, 2009.

Broder, T., Blodau, C., Biester, H., Knorr, K.-H.: Peat decomposition records in three pristine ombrotrophic bogs in southern Patagonia, Biogeosciences, 9, 1479–1491, 2012.

Bubier, J. L., Moore, T. R., Bellisario, L., Comer, N. T., Crill, P. M.: Ecological controls on methane emissions from a Northern Peatland Complex in the zone of discontinuous permafrost, Manitoba, Canada, Glob Biogeochem Cycles, 9(4), 455–470, 1995.

15   Burger, M., Berger, S., Spangenberg, I., Blodau, C.: Summer fluxes of methane and carbon dioxide from a pond and floating mat in a continental Canadian peatland, Biogeosciences, 13, 3777–3791, 2016.

Conrad, R.: Quantification of methanogenic pathways using stable carbon isotopic signatures. A review and a proposal, Org Geochem, 36(5), 739–752, 2005.

Corbett, J. E., Tfaily, M. M., Burdige, D. J., Cooper, W. T., Glaser, P. H., Chanton, J. P.: Partitioning pathways of CO_2 production in peatlands with stable carbon isotopes, Biogeochemistry, 114(1-3), 327–340, 2013.

Dorodnikov, M., Knorr, K.-H., Kuzyakov, Y., Wilmking, M.: Plant-mediated CH_4 transport and contribution of
25   photosynthates to methanogenesis at a boreal mire: a ^{14}C pulse-labeling study, Biogeosciences, 8(8), 2365–2375, 2011.

Gray, A., Levy, P. E., Cooper, M. D. A., Jones, T., Gaiawyn, J., Leeson, S. R., Ward, S. E., Dinsmore, K. J., Sheppard, L. J., Ostle, N. J., Evans, C. D., Burden, A., Zielinski, P.: Methane indicator values for peatlands: a comparison of species and functional groups, Glob Change Biol, 19, 1141–1150, 2013.

Hesslein, R. H.: Insitu Sampler for close interval pore water studies, Limnol Oceanogr, 21(6), 912–914, 1976.

Hornibrook, E. R. C., Longstaffe, F. J., William, F. S.: Evolution of stable carbon isotope compositions for methane and carbon dioxide in freshwater wetlands and other anaerobic environments, Geochim Cosmochim Acta, 64(6), 1013–1027, 2000.

5 Hornibrook, E. R. C., Bowes, H. L.: Trophic status impacts both the magnitude and stable carbon isotope composition of methane flux from peatlands, Geophys Res Lett, 34(21), 2007.

Hornibrook, E. R. C.: The stable carbon isotope composition of methane produced and emitted from northern peatlands. Andrew J. Baird, Lisa R. Belyea, Xavier Comas, A. S. Reeve und Lee D. Slater (Ed.): Carbon Cycling in Northern
10 Peatlands, Bd.184. Washington, D. C.: American Geophysical Union (Geophysical Monograph Series), pp. 187–203, 2009.

Kammann, C., Grünhage, L., Jäger, H.-J.: A new sampling technique to monitor concentrations of CH_4, N_2O and CO_2 in air at well-defined depths in soils with varied water potential, Eur J Soil Sci, 52, 297–303, 2001.

15 Klüpfel, L., Piepenbrock, A., Kappler, A., Sander, M.: Humic substances as fully regenerable electron acceptors in recurrently anoxic environments, Nat Geosci, 7, 195–200, 2014.

Knorr, K.-H., Oosterwoud, M. R., Blodau, C.: Experimental drought alters rates of soil respiration and methanogenesis but not carbon exchange in soil of a temperate fen, Soil Biol Biochem, 40(7), 1781–1791, 2008.
20
Kuiper, J. J., Mooij, W. M., Bragazza, L., Robroek, B. J. M.: Plant functional types define magnitude of drought response in peatland CO_2 exchange, Ecology, 95(1), 123–131, 2014.

Lansdown, J. M, Quay, P. D., King, S. L.: CH_4 production via CO_2 reduction in a temperate bog: A source of ^{13}C-depleted
25 CH_4, Geochim Cosmochim Acta, 56(9), 3493–3503, 1992.

Larmola, T., Bubier, J. L., Kobyljanec, C., Basiliko, N., Juutinen, S., Humphreys, E., Preston, M., Moore, T. R.: Vegetation feedbacks of nutrient addition lead to a weaker carbon sink in an ombrotrophic bog, Glob Change Biol, 19, 3729–3739, 2013.
30
Levy, P. E., Burden, A., Cooper, M. D. A., Dinsmore, K. J., Drewer, J., Evans, C., Fowler, D., Gaiawyn, J., Gray, A., Jones, S. K., Jones, T., Mcnamara, N. P., Mills, R., Ostle, N., Sheppard, L. J., Skiba, U., Sowerby, A., Ward, S. E., Zielinski, P.: Methane emissions from soils: synthesis and analysis of a large UK data set, Glob Change Biol, 18, 1657–1669, 2012.

Limpens, J., Berendse, F., Blodau, C., Canadell, J. G., Freeman, C., Holden, J., Roulet, N., Rydin, H., Schaepman-Strub, G.: Peatlands and the carbon cycle: from local processes to global implications – a synthesis, Biogeosciences, 5, 1475–1491, 2008.

5   Lund, M., Lafleur, P. M., Roulet, N. T., Lindroth, A., Christensen, T. R., Aurela, M., Chojnicki, B. H., Flanagan, L. B., Humphreys, E. R., Laurila, T., Oechel, W., Olejnik, J., Rinne, J., Schubert, P., Nilsson, M. B.: Variability in exchange of CO_2 across 12 northern peatland and tundra sites, Glob Change Biol, 16, 2436–2448, 2010.

Marushchak, M. E., Friborg, T., Biasi, C., Herbst, M., Johannson, T., Kiepe, I., Liimatainen, M., Lind, S. E., Martikainwn, P.
10 J., Virtanen, T., Soegaard, H., Shurpali, N. J.: Methane dynamics in the subarctic tundra: combining stable isotope analyses, plot- and ecosystem-scale flux measurements, Biogeosciences, 13, 597–608, 2016.

Moore, T. R., Basiliko, N.: Decomposition in Boreal Peatlands. Wieder, R. K.; Vitt, D., H.: Boreal Peatland Ecosystems, Ecol Stud, Bd.188, pp. 125–144, 2006.

Morris, P. J., Waddington, J. M., Benscoter, B. W., Turetsky, M. R.: Conceptual frameworks in peatland ecohydrology: looking beyond the two-layered (acrotelm–catotelm) model, Ecohydrology, 4, 1–11, 2011.

Murphy, K. R., Butler, K. D., Spencer, R. G., Stedmon, C. A., Boehme, J. R., Aiken, G. R.: Measurement of dissolved
20 organic matter fluorescence in aquatic environments: an interlaboratory comparison, Environ Sci Technol, 44, 9405–9412, 2010.

National Climate Data and Information Archive, 2014. Canadian Climate Normals. Dataset for the climate station Fergus, Shand Dam, 1981 to 2010. URL http://climate.weather.gc.ca/climate_normals/index_e.html (accessed November 18th,
25 2015).

Niemeyer, J., Chen, Y., Bollag, J. M.: Characterization of humic acids, composts, and peat by diffuse reflectance Fourier-Transform Infrared Spectroscopy, Soil Sci Soc Am J, 56, 135–140, 1992.

30 Ohno, T.: Fluorescence inner-filtering correction for determining the humification index of dissolved organic matter, Environ Sci Technol, 36, 742–746, 2002.

Owen, K. E., Tenhunen, J., Reichstein, M., Wang, Q., Falge, E., Geyer, R., Xiao, X. M., Stoy, P., Amman, C., Arain, A., Aubinet, M., Aurela, M., Bernhofer, C., Chojnicki, B. H., Grainer, A., Gruenwald, T., Hadley, J., Heinsch, B., Hollinger, D.,

Knohl, A., Kutsch, W., Lohila, A., Meyers, T., Moors, E., Moureaux, C., Pilegaard, K., Saigusa, N., Verma, S., Vesala, T., Vogel, C.: Linking flux network measurements to continental scale simulations: ecosystem carbon dioxide exchange capacity under non-water-stressed conditions, Glob Change Biol, 13(4), 734–760, 2007.

5 Pinsonneault, A. J., Moore, T. R., Roulet, N. T.: Effects of long-term fertilization on peat stoichiometry and associated microbial enzyme activity in an ombrotrophic bog, Biogeochemistry, 129, 149–164, 2016.

R Core Team: R: A language and environment for statistical computing, R Foundation for Statistical Computing, Vienna, 2015.

Robroek, B., Albrecht, R. J. H., Hamard, S., Pulgarib, A., Bragazza, L., Buttler, A., Jassey, V. E. J.: Peatland vascular plant functional types affect dissolved organic matter chemistry, Plant Soil, 407, 135–143, 2016.

Sander, R.: Compilation of Henry's Law Constants for Inorganic and Organic Species of Potential Importance in
15 Environmental Chemistry, Max Planck Institute of Chemistry, Mainz, 1999. Online at http://www.henrys-law.org/henry-3.0.pdf.

Schütz, H., Schroder, P., Rennenberg, H.: Role of plants in regulating the methane flux to the atmosphere, Sharkey, T.D., Holland, E.A., Mooney, H.A. (Eds.), Trace Gas Emission by Plants, Academic Press, NY, pp. 29–69, 1991.

Shannon, R. D., White, J. R.: A Three-Year Study of Controls on Methane Emissions from Two Michigan Peatlands, Biogeochemistry, 27(1), 35–60, 1994.

Strack, M., Waller, M. F., Waddington, J. M.: Sedge succession and peatland methane dynamics: A potential feedback to
25 climate change, Ecosystems, 9(2), 278–287, 2006.

Stumm, W., Morgan, J. J.: Aquatic chemistry. Chemical Equilibria and Rates in Natural Waters. 3rd ed. Hoboken: Wiley (Environmental Science and Technology)

30 Succow, M., Joosten, H.: Landschaftsökologische Moorkunde. Zweite, völlig neu bearbeitete Auflage. 2. Auflage. E. Schweizerbart`sche Verlagsbuchhandlung, Stuttgart. 2012.

Tilsner, J., Wrage, N., Lauf, J., Gebauer, G.: Emission of gaseous nitrogen oxides from an extensively managed grassland in NE Bavaria, Germany. I. Annual budgets of N_2O and NO_x emissions, Biogeochemistry, 63, 229–247, 2003.

Turetsky, M. R., Bond-Lamberty, B., Euskirchen, E., Talbot, J., Frolking, S., McGuire, M. R., Tuittila, E.-S.: The resilience and functional role of moss in boreal and arctic ecosystems, New Phytol, 196(1), 49–67, 2012.

5   van den Berg, M., Ingwersen, J., Lamers, M., Streck, T.: The role of *Phragmites* in the CH_4 and CO_2 fluxes in a minerotrophic peatland in southwest Germany, Biogeosciences, 13, 6107–6119, 2016.

Ward, S. E., Ostle, N. J., Oakley, S., Quirk, H., Henrys, P. A., Baedgett, R. D.: Warming effects on greenhouse gas fluxes in peatlands are modulated by vegetation composition, Ecol Lett, 16, 1285–1293, 2013.

Wang, M., Larmola, T., Murphy, M. T., Moore, T. R., Bubier, J.: Stoichiometric response of shrubs and mosses to long-term nutrient (N, P and K) addition in an ombrotrophic peatland, Plant Soil, 400, 403–416, 2016.

Weishaar, J. L., Aiken, G. R., Bergamischi, B. A., Fram, M. S., Fujii, R., Mopper, K.: Evaluation of specific ultraviolet

15   absorbance as an indicator of the chemical composition and reactivity of dissolved organic carbon, Environ Sci Technol, 37, 4702–4708, 2003.

Whalen, S. C., Reeburgh, W. S., Sandbeck, K. A.: Rapid methane oxidation in a landfill cover soil, Appl Environ Microbiol, 56, 3405–3411, 1990.

Whalen, S. C.: Biogeochemistry of methane exchange between natural wetlands and the atmosphere, Environ Eng Sci, 22, 73–94, 2005.

Whiting, G. J., Chanton, J. P.: Control of the diurnal pattern of the methane emission from emergent aquatic macrophytes by

25   gas transport mechanisms, Aquat Bot, 54, 237–253, 1996.

Wickland, K. P., Neff, J. C., Aiken, G. R.: Dissolved organic carbon in Alaskan boreal forest: sources, chemical characteristics, and biodegradability, Ecosystems, 10, 1323–1340, 2007.

30   Wu, Y., Blodau, C., Moore, T. R., Bubier, J., Juutinen, S., Larmola, T.: Effects of experimental nitrogen deposition on peatland carbon pools and fluxes: a modelling analysis, Biogeosciences, 12, 79–101, 2015.
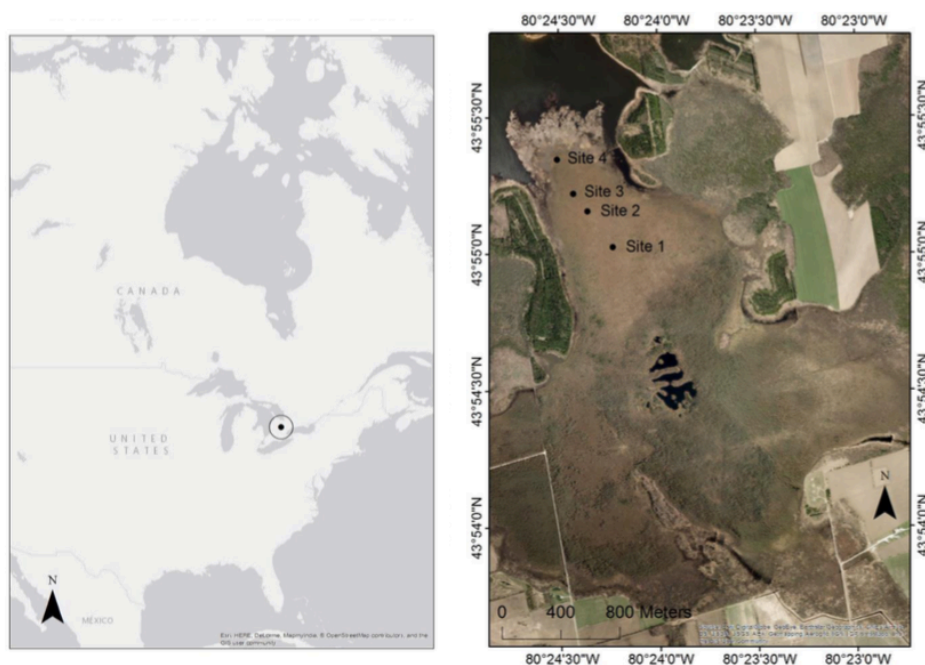
Figure 1: Location of Wylde Lake peatland complex in North America (left), and sampling sites (black dots) within Wylde Lake peatland complex (right). Source: ArcGIS.
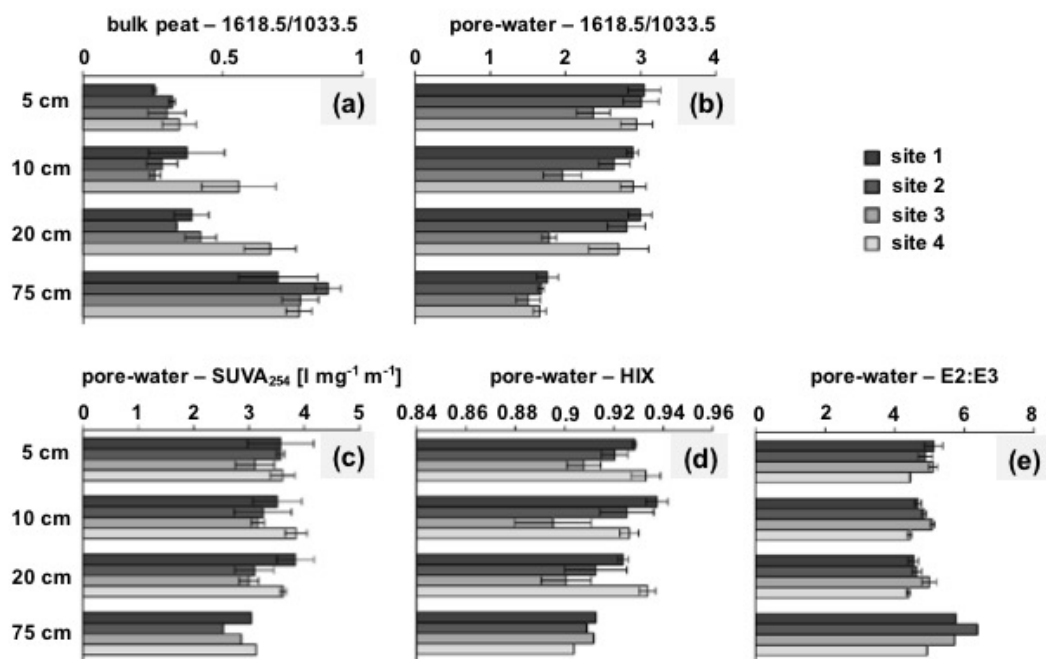
Figure 2: FTIR ratios 1618.5/1033.5 in bulk peat (a) and pore-water (b) as well as $SUVA_{254}$, indicating aromaticity, (c), HIX, humification index, (d) and E2:E3, indicative of molecular size and aromaticity, (e) for pore-water samples of the sites 1 to 4. n = 3. Error bars indicate +/- standard deviation.
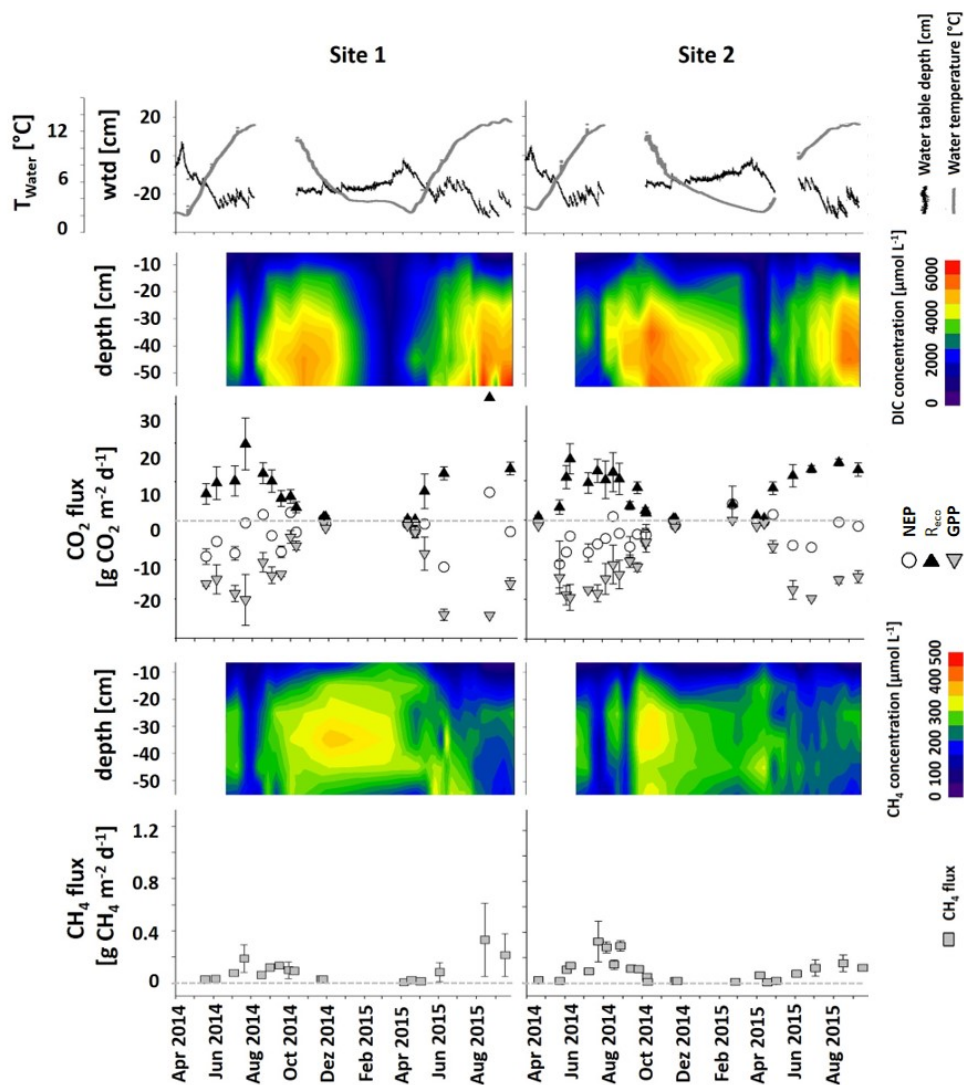
Figure 3: Development of T_{water} [° C], wtd [cm] mean DIC and mean CH_4 concentrations [μmol L^{-1}], CO_2 fluxes (NEP partitioned into R_{eco} and GPP) [g CO_2 m^{-2} d^{-1}], CH_4 fluxes [g CH_4 m^{-2} d^{-1}] ± 1 SD (n=6) in hollows of the sites 1 and 2 from April 1st, 2014 through September 22nd, 2015. Negative CO_2 and CH_4 fluxes indicate uptake, positive fluxes indicate a release to the atmosphere.
5 **Dashed gray lines in the flux graphs indicate a 0-flux.**
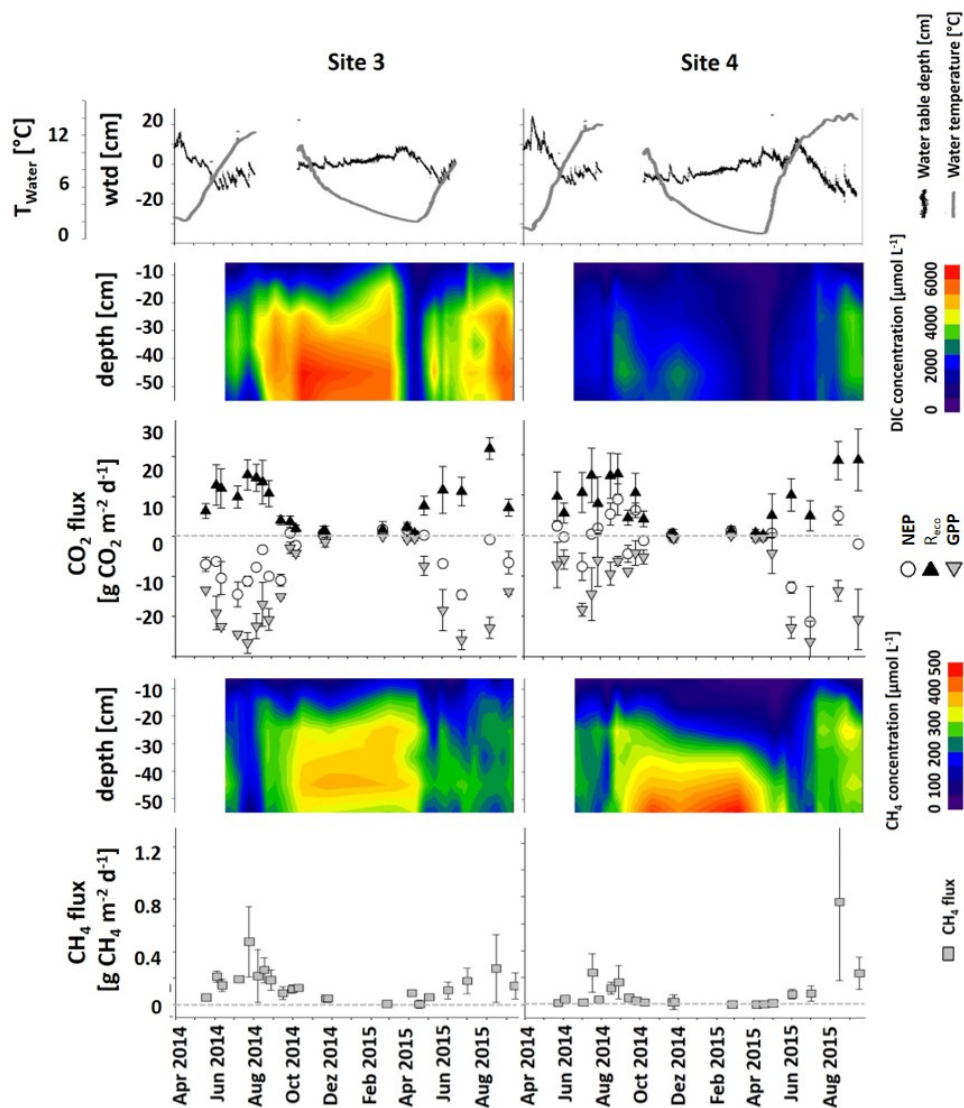
Figure 4: Development of T_{water} [° C], wtd [cm] mean DIC and mean CH_4 concentrations [μmol L^{-1}], CO_2 fluxes (NEP partitioned into R_{eco} and GPP) [g CO_2 m^{-2} d^{-1}], CH_4 fluxes [g CH_4 m^{-2} d^{-1}] ± 1 SD (n=6) in hollows of the sites 3 and 4 from April 1st, 2014 through September 22nd, 2015. Negative CO_2 and CH_4 fluxes indicate uptake, positive fluxes indicate a release to the atmosphere.
5   **Dashed gray lines in the flux graphs indicate a 0-flux.**
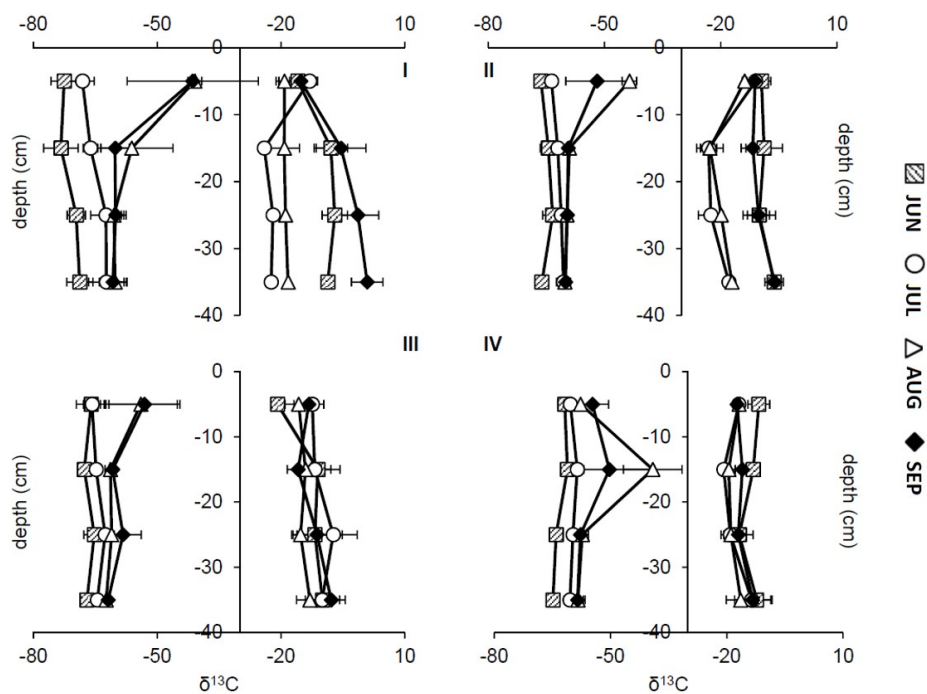
Figure 5: Profiles of δ¹³C-CH₄ (left) and δ¹³C-CO₂ (right) signatures at sites 1-4 in the peat in 5-35 cm depth at different points in time. Squares = June (06/11), circles = July (07/08), triangles = August (08/27), diamonds = September (09/17). Graphs show mean values and standard deviations from three replications at each site. n = 1-3.
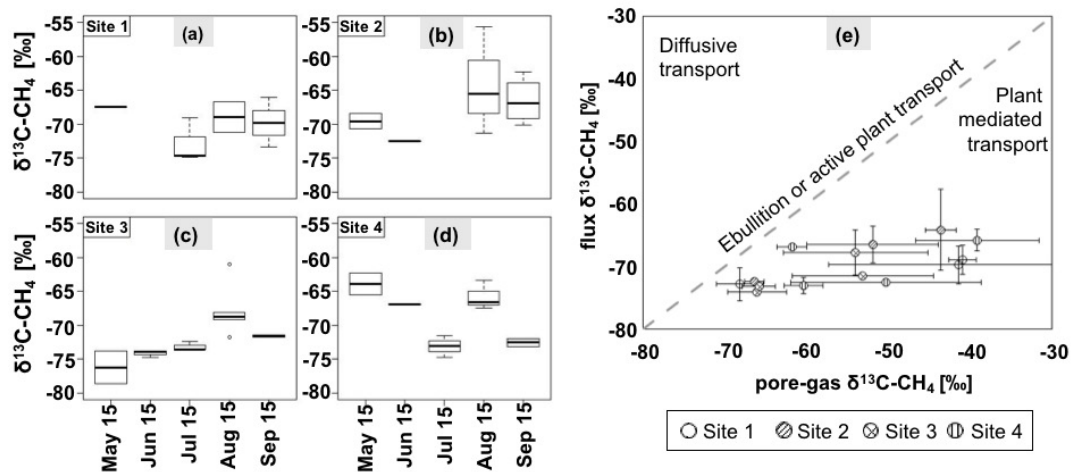
Figure 6: δ^{13}C-CH$_4$ signatures (‰) of CH$_4$ fluxes from May to September for the sites 1 (a), 2 (b), 3 (c) and 4 (d). n = 1-4. In July 2015, sampling at site 2 was not possible. Bold lines are the median, boxes show the 25 and 75 percentile, whiskers indicate minima and maxima within 1.5 times the interquartile range. Single points show outlier. (e): dominant flux pathway of CH$_4$ according to (Hornibrook, 2009). Empty circles = site 1, cicrles with diagonal lines = site 2, circles with crosses = site 3, circles with vertical lines = site 4. Dashed line represents transport via ebullition or active plant transport without any isotopic fractionation. Values are means of pore-gas samples from 5 cm depth and chamber flux measurements.), diamonds = September (09/17). Graphs show mean values and standard deviations from three replications at each site. n = 1-3.

Table 1: Overview of study sites' hollow properties within Wylde Lake peatland, including coverages of dominant plant functional types (PFT), peat age at 60 cm depth ± 1 SD (n=3), pH, stochiometric ratios (C/N, C/P, N/P, C/Ca, C/Mg, C/K) at the peat surface ± 1 SD (n=3). Stoichiometric ratios have been presented in Berger et al., (submitted for publication).

Site	Cover			Peat age	pH		stoch. Ratios					
	Sphagn.	Gram.	Shrubs	at 60 cm	at surface	at 75 cm	C/N	C/P	N/P	C/Ca	C/Mg	C/K
	[%]	[%]	[%]	[years]								
1	100	10	8	70 (± 21)	3.6	3.7	52.6 ±4.7	1207.2 ±85.9	35.1 ±0.9	129.1 ±3.4	926.0 ±112.8	271.9 ±9.3
2	100	30	5	50 cm: 135	4.3	3.7	47.4 ±6.4	1256.4 ±50.2	41.8 ±2.5	99.1 ±11.0	1228.6 ±26.9	313.0 ±2.0
3	100	35	4	148 (± 45)	3.8	3.8	51.7 ±2.7	1403.0 ±123.0	37.6 ±2.8	146.5 ±18.1	1063.3 ±46.4	287.2 ±4.3
4	60	10	30	184 (± 17)	4.0	4.1	41.5 ±4.2	1342.6 ±244.7	45.7 ±3.4	187.8 ±11.0	962.0 ±60.3	258.9 ±7.2